Fufang Zhenshu Tiaozhi Capsule Enhances Bone Formation and Safeguards against Glucocorticoid-Induced Osteoporosis through Innovative Mekk2-Mediated β-Catenin Deubiquitination

Guoju Hong
the Third Affiliated Hospital of Guangzhou University of Chinese Medicine
Jiangyan Wang
The First Affiliated Hospital of Guangdong Pharmaceutical University
Dongdong Ge
The First Affiliated Hospital of Guangdong Pharmaceutical University
Lin Tang
The First Affiliated Hospital of Guangdong Pharmaceutical University
Li Hu
The First Affiliated Hospital of Guangdong Pharmaceutical University
Chenghong Ma
The First Affiliated Hospital of Guangdong Pharmaceutical University
Qunwei Dong
Yunfu Hospital of Traditional Chinese Medicine
Ping Sun (gdsthgj@foxmail.com)
The First Affiliated Hospital of Guangdong Pharmaceutical University

Research Article

Keywords: Osteoporosis, Medicine, Chinese Traditional, beta Catenin, MAP Kinase Kinase Kinase 2, Wnt Signaling Pathway

Posted Date: September 13th, 2023

DOI: https://doi.org/10.21203/rs.3.rs-3196641/v1

Additional Declarations: No competing interests reported.

Abstract

Background

The homeostasis of bone is reliant on the regulation of β-catenin activity in osteoblasts. Glucocorticoids (GC) have been found to reduce β-catenin activity through Wnt pathway signaling, leading to osteoporotic pathology. On the other hand, the activation of β-catenin in osteoblasts can be mediated by mitogen-activated protein kinase kinase kinase 2 (Mekk2), which presents a promising and innovative therapeutic approach to counteract GC-induced osteoporosis (GIOP). The remarkable efficacy of Fufang Zhenshu Tiaozhi (FTZ) capsules in the treatment of GC-induced osteoporosis has been established, although the underlying mechanisms of action have yet to be determined.

Methods

In this investigation, Mekk2-/- mice were generated utilizing the CRISPR/Cas9 methodology and subjected to Alcian Blue-Alizarin Red staining and immunofluorescence for assessment. To create GIOP models, Mekk2-/- and WT mice were administered dexamethasone (DXMS) and subsequently treated with FTZ. The phenotypic variations in the mice models were analyzed by Micro-CT and histomorphology evaluations. Primary osteoblasts separated from *Mekk2*$^{-/-}$ and WT mice were subjected to FTZ or WNT3a treatments. Following this, phosphorylation levels of β-catenin and Mekk2, as well as the protein expression of Runx2, were assessed using western blotting and immunoprecipitation methods. C3H10T1/2 cells, which were transfected with TOPflash-luciferase and Renilla, were treated with FTZ and Wnt3a, and β-catenin activity was determined.

Results

The administration of FTZ *in vivo* successfully averted GC-induced bone loss. Notably, this protective effect was significantly undermined in Mekk2-deficient mice. Moreover, FTZ was found to effectively promote the process of osteogenic differentiation in primary osteoblasts by modulating the expression of Mekk2. It is noteworthy that the effects of FTZ on Mekk2 are mediated via a mechanism that operates independently of the Wnt signaling pathway. Furthermore, FTZ has been shown to enhance the process of β-catenin deubiquitination, thus further contributing to its beneficial effects on bone health.

Conclusions

The present study posits that FTZ exerts a remarkable safeguarding effect on bone mass in the context of glucocorticoid-induced osteoporosis (GIOP). The mechanism through which FTZ confers this benefit involves the activation of Mekk2/β-catenin signaling pathways, which represents a promising alternative strategy to counteract the deleterious effects of GIOP by augmenting osteoblastogenesis.

1. Background

Glucocorticoid-induced osteoporosis (GIOP) is a complex bone metabolism disorder that arises due to prolonged or high-dose glucocorticoid (GC) therapy[1,2]. This condition is characterized by a rise in serum free fatty acids, reduced bone mass accompanied by microstructural abnormalities, and an increased risk of bone fragility and fracture[2–4]. Epidemiological studies have indicated that approximately 4.6% of osteoporotic women globally receive GC therapy[5,6]. Moreover, up to 50% of patients receiving GC for chronic diseases, particularly postmenopausal women, are susceptible to developing osteoporosis. The pathogenesis of GIOP is multifactorial and remain s incompletely understood. Notably, the ubiquitination of β-catenin has emerged as a critical molecular mechanism underlying GC-induced osteoporosis[7]. GC therapy impairs the classical Wnt-β-catenin pathway by enhancing the phosphorylation and ubiquitination of β-catenin and promoting its proteasomal degradation, which ultimately inhibits osteoblast differentiation[7,8]. While preventing β-catenin degradation has been identified as a viable strategy for promoting osteoblastogenesis, there are currently no approved therapies targeting this pathway.

Recent research has identified mitogen-activated protein kinase kinase kinase 2 (Mekk2) as a novel regulator of β-catenin ubiquitination, which operates through a non-classical pathway that stabilizes β-catenin and promotes osteoblast differentiation[9,10]. The Mekk2 pathway is independent of the canonical Wnt-β-catenin signaling pathway. Specifically, Mekk2 activation at serine 675 triggers the recruitment of ubiquitin carboxyl-terminal hydrolase 15 (USP15), which removes ubiquitin from β-catenin and prevents its protease-dependent turnover. Unlike the classical Wnt pathway, the Mekk2 pathway enhances the deubiquitination process of β-catenin, thereby promoting its stabilization and osteoblast differentiation[9,11,12]. Therefore, targeting Mekk2 may represent a safer approach to treating GIOP than targeting the Wnt pathway.

Traditional Chinese medicine, including the Fufang Zhenshu Tiaozhi capsule (FTZ), has shown promise as an alternative therapy for preventing osteoporosis[13,14]. FTZ, a commercial Chinese herbal medicine, has been found to possess hyperlipidemia regulatory[15], anti-aging[16], and anti-atherosclerotic[17], anti-type 2 diabetes mellitus[18] properties. Additionally, FTZ has been shown to protect against age-related osteoporosis in mice by rebalancing the metabolisms of sphingolipids, glycerophospholipids, and amino acids[14]. However, the mechanisms underlying its beneficial effects in GIOP have yet to be fully elucidated. Here, we hypothesize that FTZ may prevent GC-induced bone loss and promote osteoblastic activity by modulating MEKK2-mediated phosphorylation of β-catenin.

2. Method

2.1 Reagents

The commercial FTZ utilized in this study was procured from Zhixin Chinese Herbal Medicine Co., Ltd. located in Guangzhou, P.R. China. The FTZ is composed of a synergistic blend of herbal ingredients, namely Fructus Ligustri Lucidi (Nvzhenzi), Coptis Rhizome (Huanglian), Salvia miltiorrhiza (Danshen), Panax pseudo-ginseng (Sanqi), Atractylodes lancea (Cangzhu), Cirsium japonicum Fisch. ex DC. (Daji), Citrus medica L. var.sarcodactylis Swingle (Foshou), and Eucommia ulmoides (Duzhong)[14]. These herbs were subjected to an alcohol extraction process and were produced as previously reported[19]. The quality of the FTZ extract was evaluated by high-performance liquid chromatography (HPLC) fingerprinting, following a previously established protocol[19,20].

C57BL/6 mice used in this study were either procured from the Experimental Animal Center of Guangzhou University of Chinese Medicine located in Guangzhou, P.R. China or obtained from Shanghai Model Organism Center Lnc. located in Shanghai, P.R. China. The animal experiments conducted in this study were in compliance with the ARRIVE guidelines and were carried out following the UK Animals (Scientific Procedures) Act, 1986, and associated guidelines, EU Directive 2010/63/EU. The culture media, including α-MEM and FBS, were purchased from Gibco (Carlsbad, CA, USA). Recombinant mouse Wnt3a protein was obtained from R&D Systems, located in Minneapolis, MN, USA.

2.2 Generation of *Mekk2*$^{-/-}$ mouse model

The manipulation of *Mekk2* gene and its subsequent q-PCR validation were outsourced to Shanghai Model Organism Center Lnc. in Shanghai, P.R. China. Nonhomologous recombination using CRISPR/Cas9 was employed to create a *Mekk2* frameshift mutation, as illustrated in **Fig. S1**. The Cas9 mRNA and gRNA were transcribed in vitro with the mMESSAGE mMACHINE T7 Ultra Kit (Ambion, TX, USA) as per the manufacturer's protocol. F0 mice were produced after injecting Cas9 mRNA and gRNA into fertilized eggs of C57BL/6J mice, as depicted in **Fig. S2A**. The Mekk2 mutation in the F0 mice was confirmed by PCR (**Fig. S2B**). A total of eight F0 mice with the target gene frameshift mutation were generated. Subsequently, positive F0 mice were selected for mating with wild-type (WT) C57BL/6J mice to obtain F1 heterozygous *Mekk2*$^{-/-}$ mice. Primary osteoblasts were extracted from the crania of the F1 newborn mice, and knockout F1 mice aged 6–8 weeks were used to establish the GIOP model.

2.3 GIOP model establishment by *Mekk2*$^{-/-}$ and WT mice

Specific-pathogen-free WT C57BL/6 mice, both male and female in equal proportions, aged 6–8 weeks and weighing 18–20 g, were procured to ensure parity with the number of Mekk2-/- mice. The mice were maintained under controlled conditions, with a temperature of 25°C, a humidity level of 50–60%, and a 12/12 h light/dark cycle. Food and water were provided ad libitum.

WT and *Mekk2*$^{-/-}$ mice, aged between 6 to 10 weeks, were allocated to four groups using a complete randomized design: WT group, WT + dexamethasone (DXMS) group, WT + DXMS + FTZ group, and *Mekk2*$^{-/-}$+DXMS + FTZ group (n = 8 per group). DXMS was administered intramuscularly twice weekly for 12 weeks at a dose of 0.2 mg/100 g body weight[21]. In the groups treated with FTZ, FTZ (3 g/kg) was orally administered in mice twice daily for 12 weeks[14]. In groups without FTZ treatment, 1 mL of saline

water was infused into the stomach of mice twice daily instead. After 6 weeks of treatment, the mice were euthanized and the bilateral tibias were extracted and stored at − 80°C until further analysis. Mice with reduced food intake or exhibiting anxiety after FTZ treatment or dying for unknown reasons were excluded from the study. Euthanasia was performed via cervical dislocation after the rapid induction of unconsciousness caused by an overdose of carbon dioxide (CO_2). The first author conducted the entire study under a double-blind design, and the other group members responsible for drug treatment were unaware of the group allocation.

2.4 Alcian Blue-Alizarin Red staining of fetuses

Three fetuses each from *Mekk2*$^{-/-}$ and WT gravid mice were obtained after 13 days of pregnancy and euthanized humanely. The fetuses were then stained with Alcian Blue-Alizarin Red solution for 4 hours. Next, the samples were soaked in 1% potassium hydroxide for 24 to 36 hours to visualize the skeleton and muscles. Finally, the samples were stored in 50% glycerin and prepared for imaging.

2.5 Immunofluorescence testing

The tibial samples from both *Mekk2*$^{-/-}$ and WT mice (n = 8) were collected for immunofluorescence testing. The tissue sections were prepared and underwent a series of washing steps using xylene I, xylene II, anhydrous ethanol I, anhydrous ethanol II, 85% alcohol, and 75% alcohol, followed by washing with distilled water. The sections were then subjected to heat retrieval using a retrieval box filled with 10% ethylenediaminetetraacetic acid soaking solution and a microwave. After cooling, the sections were washed with phosphate-buffered saline (PBS, pH 7.4) and blocked with bovine serum albumin for 30 min. Anti-MEKK2 (Abcam, Cambridge, UK) was added to the sections, which were incubated overnight at 4°C. Following washing with PBS, the sections were incubated with FITC-labeled secondary antibody (1:200, Biodragon, Beijing, P.R. China) at room temperature for 50 min in the absence of light, followed by a 10-min incubation with DAPI solution (Solarbio, Beijing, P.R. China). Finally, the sections were observed under a fluorescence microscope, and the images were captured using different excitation and emission wavelengths for DAPI and FITC (DAPI: excitation wavelength: 330–380 nm, emission wavelength: 420 nm; FITC: excitation wavelength: 465–495 nm, emission wavelength: 515–555 nm).

2.6 Micro-CT

After removing soft tissues, the proximal tibias (n = 8) were mounted on a micro-CT platform (Scanco Medical, Wangen-Brüttisellen, Switzerland) and scanned to obtain two- and three-dimensional images. Structural parameters within a square region of interest (ROI) established at a distance of 0.5 mm from the tibia growth plate were analyzed using the CTAN program (Bruker micro-CT, Kontich, Belgium). Bone volume per tissue volume (BV/TV), trabecular thickness (Tb.Th), number of trabeculae (Tb.N), and connectivity density (Conn.Dn) were measured within the ROI to determine the structural parameters of interest.

2.7 Histological and histomorphometric analysis

Following micro-CT analysis, specimens (n = 8) were harvested, fixed, decalcified using a 10% ethylenediaminetetraacetic acid (EDTA) soaking solution for a duration of 3 weeks until they achieved a softened consistency. The specimens were then embedded into paraffin blocks for subsequent sectioning and staining. Specifically, the tibias were sectioned into 4 μm thick sections using a microtome. For histological evaluation, hematoxylin and eosin (H&E) staining was performed on the sections, which were analyzed under a microscope.

2.8 Isolation and culture of osteoblast

Primary cells were obtained from the calvaria of 5-day-old wild-type (WT) or Mekk2-/- mice using collagenase II digestion. Subsequently, the cells were cultured in osteogenic induction medium (OIM) consisting of 0.1 mM dexamethasone, 50 mM L-ascorbic acid-2-phosphate, and 10 mM β-glycerophosphate to stimulate differentiation into osteoblasts for 21 days. Primary osteoblasts were cultured in α-MEM medium supplemented with 10% fetal bovine serum (FBS), 2 mM L-glutamine, 1% penicillin/streptomycin, 1% Hepes, and 1% nonessential amino acids.

2.9 Preparation of FTZ-containing serum

The mice underwent a 7-day acclimation period to the laboratory environment and were subjected to a 6-hour fast prior to FTZ administration. The FTZ capsules, each containing 0.6 g/kg, were administered to the mice twice daily for 7 consecutive days. One hour following the final administration, mice were anesthetized and blood was drawn from their hearts. The blood samples were left to stand at room temperature for 30 minutes and then centrifuged at 3000 rpm for 15 minutes. The resultant supernatant, which contained the FTZ compound, was collected and stored at a temperature of -80°C for further usage.

2.10 MTT assay

To assess cell proliferation following FTZ treatment, the 3-[4,5-dimethylthiazol]-2, 5-diphenylterazolium bromide (MTT) assay was utilized. In brief, osteoblasts were isolated and seeded in 96-well plates at a density of 5×103 cells per well. Upon reaching confluence, the cells were treated with 7.5% (v/v) FTZ-containing serum. 20μL MTT was added to each well at specific time points (1, 3, 5, 7, and 14 days), followed by incubation at 37°C for an additional 4 hours. Thereafter, the plate was measured using a microplate reader (Bio-Rad, model 550, Hercules, CA, USA) to determine the extent of cell proliferation.

2.11 Staining of isolated primary cells

To conduct Von Kossa staining analysis, the isolated cells from each group were first treated with 10% neutral formalin buffer for fixation, followed by exposure to 2.5% Von Kossa silver nitrate (Solarbio, Beijing, P.R. China) for staining. Alizarin Red staining was performed by fixing the cells with 4% PFA for 30 minutes, then washing with phosphate-buffered saline (PBS) before adding a 0.2% Alizarin Red Tris HCl (PH: 8.3) solution into the wells for 5 minutes. To measure the Alkaline Phosphatase (ALP) activity of osteoblasts, cells were cultured similarly to the Alizarin Red staining procedure, followed by fixation with

95% alcohol, washing with PBS three times, and stained using the BCIP/NBT Alkaline Phosphatase Color Development Kit (Beyotime, Shanghai, P.R. China) according to the manufacturer's instructions.

2.12 Quantitative reverse-transcription polymerase chain reaction (qRT-PCR)

The mRNA levels of specific genes of OIM-induced osteoblasts were assessed using qRT-PCR. To be specific. total RNA was extracted using TRIZOL® reagent (Life Technologies, Carlsbad, CA, USA). Subsequently, reverse transcription was performed using a Reverse Transcription Assisted First Strand cDNA Synthesis Kit. qRT-PCR was conducted using SYBR Green PCR Master Mix, and the expression levels were normalized using *Gapdh* as a reference gene. The Comparative Ct (ΔCt) method was employed for data analysis. The primer sequences utilized for gene amplification are provided in Table 1.

Table 1
Sequences of both the forward and reverse primers of mRNAs in qRT-PCR.

Gene	Forward	Reverse
m-Runx2	5'-TGGCTTGGGTTTCAGGTTAG-3'	5'-GGTTTCTTAGGGTCTTGGAGTG-3'
m-Alp	5'-CTTTCGTAGCAGCAGCAAAC-3'	5'-GGAGCGCGTCTTGGATATT-3'
m-Col1a1	5'-AGACCTGTGTGTTCCCTACT-3'	5'-GAATCCATCGGTCATGCTCTC-3'
m-Sp7	5'-TGGAGAGGGAAAGGGATTCT-3'	5'-GAAATCTACGAGCAAGGTCTCC-3'
m-Bglap	5'-CTGCCCTAAAGCCAAACTCT-3'	5'-AGCTGCTGTGACATCCATAC-3'
m-β-actin	5'-GAGGTATCCTGACCCTGAAGTA-3'	5'-CACACGCAGCTCATTGTAGA-3'

2.13 Western blotting and immunoprecipitation

Osteoblast lysates derived from cells isolated from wild-type (WT) and Mekk2-deficient mice were stimulated with phosphate-buffered saline (PBS) or a 7.5% (v/v) concentration of fetal thymus zinc (FTZ)-containing serum (diluted to 10% in fetal bovine serum (FBS)) at specific time points. The resultant lysates were mixed with radioimmunoprecipitation assay lysis buffer (Millipore, Burlington, MA, USA), which contained a protease and phosphatase inhibitor cocktail. The proteins in the lysates were separated using 10% sodium dodecyl sulfate-polyacrylamide gel electrophoresis and subsequently transferred onto a polyvinylidene fluoride membrane (GE healthcare, Chicago, IL, USA). The membrane was then blocked with 5% skimmed milk for an hour. Next, the membrane was subjected to incubation with primary antibodies, including anti-phosphorylated β-catenin, anti-β-catenin, and anti-Runx2 (Sigma-Aldrich, St. Louis, MO, USA), overnight. Following overnight incubation, the membrane was washed with 1× tris-buffered saline containing 0.1% Tween® 20 and then incubated with corresponding secondary antibodies. Finally, the membrane was exposed to capture images of protein bands.

To perform immunoprecipitation, osteoblasts were lysed and the resulting lysates were incubated with Mekk2-conjugated agarose beads (Abcam, Cambridge, UK) overnight at 4℃. The beads were then washed thrice to remove any non-specifically bound proteins and the immunoprecipitates were eluted with Laemmli sample buffer, followed by analysis via blotting techniques.

2.14 Luciferase reporter experiment

To explore the transcriptional activity of β-catenin, C3H10T1/2 cells (a murine mesenchymal stem cell line generously provided by the Lab of Prof. Ping Sun) were grown on 12-well plates and transfected with TOPflash plasmid (0.5 μg) and plasmid expressing Renilla luciferase (50 ng) in a transient manner. Subsequently, after 12 hours, the cells were treated with 7.5% (v/v) FTZ-containing serum, 100 ng/mL of recombinant Wnt3a, or both in serum-free medium. After 24 hours, the cells were washed with phosphate-buffered saline (PBS) in shaking and lysed. The luciferase activity was measured using a Dual-Luciferase Reporter assay System (Promega, Madison, WI, USA).

2.15 Statistical analysis

All experimental procedures conducted in this study were performed thrice, independently, to ensure the reproducibility and accuracy of the results. The data were presented as mean ± standard deviation (SD). Statistical analysis was performed utilizing SPSS 22.0. The inter-group comparisons were carried out using one-way analysis of variance (ANOVA), and the significance level was set at $P < 0.05$. Any difference with a *P*-value lower than 0.05 was considered statistically significant.

3 Results

3.1 Phenotype of *Mekk2*$^{-/-}$ mouse

The Alcian Blue-Alizarin Red staining technique was employed to evaluate the impact of Mekk2 on bone loss prevention *in vivo* in both wild-type (WT) and *Mekk2*-deficient (*Mekk2*$^{-/-}$) mice. Notably, the total bone mass was markedly diminished in the knockout mice relative to their WT counterparts, which was accompanied by shortened and slimmed limbs and ribs (as illustrated in Fig. 1A). The immunofluorescence staining assay was conducted to detect the expression of Mekk2 in the proximal tibia of WT and *Mekk2*$^{-/-}$ mice. The outcomes unveiled robust green fluorescence signals at the surface of the bone trabeculae adjacent to the epiphysis of WT mice; conversely, no fluorescence was observed in the corresponding section of the knockout mice (as shown in Fig. 1B). These findings align with the prior study[9] and underscore the regulatory role of MEKK2 in maintaining bone homeostasis *in vivo*.

3.2 The inhibitory effects of FTZ on GC-induced bone loss in *Mekk2*$^{-/-}$ mice

To assess the efficacy of FTZ in mitigating glucocorticoid (GC)-induced osteoporosis, wild-type (WT) and *Mekk2*-deficient (*Mekk2*$^{-/-}$) mice were subjected to GC administration and subsequently treated with

either FTZ (at a dosage of 3 mg/kg) or saline solution. No untoward incidents were observed during the course of the experiment. Micro-computed tomography (micro-CT) analysis revealed that FTZ treatment significantly augmented bone volume/total volume (BV/TV), trabecular number (Tb.N), and trabecular thickness (Tb.Th), which indicates a reduction in GC-induced bone loss. However, in *Mekk2*$^{-/-}$ mice, the beneficial impact of FTZ was impeded, suggesting that the antagonistic effects of FTZ against GC-induced osteoporosis are mediated by Mekk2 (Fig. 2A–E). The histological analysis, as demonstrated by BV/TV and bone surface (BS), was consistent with the micro-CT findings, thus providing evidence that FTZ mitigated GC-induced osteoporosis via Mekk2 (Fig. 3A–C).

3.3 Promotion of osteoblast differentiation by FTZ via MEKK2

To determine the direct impact of FTZ-containing serum on primary osteoblast proliferation in WT mice, an MTT assay was conducted. Our results revealed a significant promotion of cell proliferation in the presence of FTZ, with effects sustained for up to 14 days (Fig. 4A).

The potential of FTZ to induce osteoblast differentiation was first assessed via the Von Kossa assay. After 7 days, bone nodules were observed in osteoblasts isolated from WT mice, whereas few bone nodules were detected in cells from *Mekk2*$^{-/-}$ mice. In cells isolated from FTZ-treated *Mekk2*$^{-/-}$ mice, the number of bone nodules was slightly lower than that of the WT mice (Fig. 4B). Moreover, Alizarin Red staining showed that there was a notable difference between the WT + DXMS + FTZ group and the *Mekk2*$^{-/-}$+DXMS + FTZ group in terms of mineralized nodule formation. The effects of FTZ on nodule formation in *Mekk2*$^{-/-}$ osteoblasts were weaker than in WT osteoblasts (Fig. 4C, D). Additionally, FTZ was observed to increase alkaline phosphatase (ALP) activity (Fig. 4E, F). Taken together, these findings indicate that FTZ can promote osteogenic differentiation through Mekk2, although its effects are not solely mediated by this factor.

3.4 In *vitro* FTZ promotes the expression of osteoblast marker genes through *Mekk2*

Osteoblast differentiation is associated with regulation of marker genes in response to OIM. We made further analysis of the activation of FTZ on osteoblast differentiation by assessing the mRNA expression levels of the OIM-inducible osteoblast marker genes, such as *Runx2*, *Col1a1*, *Alp*, *Sp7*, *Bgalp*. As shown by RT-PCR, FTZ dramatically triggered the expression of genes. Conversely, the knockout of *Mekk2* essentially restrained the expression of majority of osteoclast marker genes. Thus, by these findings, FTZ the expression of osteoclast marker genes in *vitro* through *Mekk2* (Fig. 5).

3.5 FTZ activated Mekk2 and stabilized β-catenin in osteoblasts

To evaluate the influence of FTZ-containing serum on the Mekk2 pathway in osteoblasts, we employed OIM to stimulate the osteogenic differentiation of cells isolated from WT mice or *Mekk2*$^{-/-}$ mice, and the phosphorylation of β-catenin was assessed through Western blot analysis. Our results revealed that FTZ significantly enhanced the phosphorylation of β-catenin at 60 mins compared with the PBS control. However, in the corresponding FTZ-treated osteoblasts isolated from *Mekk2*$^{-/-}$ mice, the phosphorylation of β-catenin was maintained at a low level, albeit still slightly higher than that observed in the PBS-treated cells (Fig. 6A–C). FTZ notably induced the activation of Mekk2 to a greater extent than Wnt3 in WT mouse cells, which suggests that FTZ acts independently of the Wnt/β-catenin pathway by exerting its effects on Mekk2 (Fig. 6D, E). Remarkably, both FTZ and Wnt3a increased the expression of RUNX2 (Fig. 6F, G). In the luciferase gene reporter assay of C3H10T1/2 cells, the β-catenin activity upon addition of FTZ and Wnt3a was substantially higher than those observed with FTZ or Wnt3a alone (Fig. 6H).

4. Discussion

The incidence and development of GIOP are determined largely by the intricate balance between osteoblastic bone formation and osteoclastic bone resorption[22–24]. Thus, it is imperative to develop therapeutic strategies to restore the biofunctions of osteoblasts[25,26]. The binding of GCs to the glucocorticoid receptor (also known as NR3C1) can suppress osteoblastogenesis and promote osteocyte and mature osteoblast apoptosis[27]. Recently, emerging therapies have been proposed for the treatment of GIOP that counteract the effects of GC administration. The updated guideline of the American College of Rheumatology (ACR) recommends lifestyle changes, such as balanced diet, body weight control, smoking cessation, limited alcohol consumption, and active exercise, as well as calcium supplementation, to attenuate the adverse effects of GCs on the musculoskeletal system[28]. Bisphosphonates are the first-line oral medications used in clinical practice for the treatment of GIOP[29]. They have been shown to significantly enhance osteoblast proliferation and downregulate osteocyte apoptosis[30]. Denosumab has been shown to be beneficial for maintaining bone matrix in the lumbar vertebra and hip in patients with GIOP compared to bisphosphonates, according to a meta-analysis study[31]. However, the safety of these drugs is still a matter of debate, and undesirable side effects such as osteonecrosis of the jaw have been reported[30,32]. Therefore, the safety of these drugs remains questionable, and novel safe and effective treatments are urgently needed. Fufang Zhenshu Tiaozhi capsule, the most representative Chinese herbal medicine, has demonstrated protective effects against age-related osteoporosis *in vivo*, suggesting its potential as a therapeutic agent for bone loss diseases[16].

The Wnt/β-catenin signaling pathway has been identified as the primary target of GCs, closely associated with the onset of osteoporosis[1,33]. GCs have been shown to expedite β-catenin phosphorylation and degradation via the inhibition of the Wnt/β-catenin pathway, thereby inducing the ubiquitination of β-catenin as the general mechanism leading to GIOP[8,34]. Despite the known involvement of β-catenin signaling dysfunction in GIOP, there are currently no approved therapeutic agents or drugs capable of blocking the Wnt/β-catenin pathway. The lack of such therapeutic interventions highlights the significant

challenges that complicate drug development in this context, including the abundance of Wnts and their cognate receptors, and the unexpected phenotypes that arise from dysregulation of the Wnt/β-catenin signaling pathway[7].

Mekk2, a constituent of the Mekk/Set11 protein subfamily, is presumed to promote osteoblast differentiation and prevent bone loss. As a potent activator of the JNK signaling pathway, Mekk2 activates ERK1/2, ERK5, and p38, as well as other MAPK factors, thereby affecting the proliferation, differentiation, and apoptosis of osteoblasts[35]. Suppression of SMAD Specific E3 Ubiquitin Protein Ligase 1 (Smurf1) activity results in the accumulation of phosphorylated Mekk2 and JNK signaling, leading to reduced osteoblast activity[10]. Conversely, Cadherin-1 inhibits Smurf1 expression while activating Mekk2 signaling, subsequently promoting osteoblast differentiation[36]. Furthermore, recent research indicates that Mekk2 promotes the deubiquitination of β-catenin through an alternative pathway[9]. Unlike the Wnt/β-catenin pathway, Mekk2 inhibits β-catenin ubiquitination by recruiting USP15 and preventing protease turnover. Mekk2's positive regulation of β-catenin stability is significant for restoring bone mass. From this viewpoint, Mekk2 is a potential alternative method for modulating β-catenin due to its critical role in FTZ-MEKK2–β-catenin signaling and its particular osteogenic functions. In this study, we generated *Mekk2* knockout mice to observe specific phenotypic changes in bone mass. The osteogenesis of *Mekk2*$^{-/-}$ mice was inferior to that of wild-type mice. Alcian Blue-Alizarin Red staining of fetuses revealed obvious delays in bone development in *Mekk2*$^{-/-}$ mice, consistent with previous findings[9].

Pharmacological interventions targeting the Mekk2 pathway hold promise for inhibiting β-catenin ubiquitination as effectively, if not more so, than other approaches. In our prior investigation, we reported that FTZ modulated the bio-metabolic processes involved in aging-related osteoporosis[14]. Based on this, we hypothesize that FTZ could augment osteogenic activity and enhance bone metabolism in the presence of GC. The present research demonstrates that FTZ significantly mitigated bone loss in GC-induced osteoporosis, but this effect was attenuated in *Mekk2*-deficient mice. The macroscopic bone changes in response to FTZ or GC exposure as visualized by micro-CT and H&E staining correlated well with the observations made using ALP and Alizarin Red staining of primary osteoblasts derived from each group. Notably, FTZ dramatically triggered the expression of genes. Conversely, the knockout of *Mekk2* essentially restrained the expression of majority of osteoclast marker genes.

Moreover, in our current investigation, we delved into the underlying mechanism of FTZ on β-catenin in primary cell lines isolated from *Mekk2*$^{-/-}$ and WT mice (Fig. 7). The phosphorylation of β-catenin in FTZ-treated osteoblasts from *Mekk2*$^{-/-}$ mice was found to be significantly lower than that of WT cells, which substantiated that FTZ stabilized β-catenin and hampered β-catenin ubiquitination in osteoblasts by Mekk2. To establish the differentiation between the FTZ–Mekk2–β-catenin axis and the Wnt/β-catenin signaling pathway, we evaluated the capacity of FTZ to instigate Mekk2 phosphorylation in primary osteoblasts from WT mice through immunoprecipitation, and contrasted the results with those of Wnt3a administration. The outcomes revealed that FTZ spurred Mekk2 phosphorylation to a greater degree than

Wnt3a. However, both FTZ and Wnt3a substantially enhanced the expression of Runx2 in WT-mice cells, a pivotal transcription factor linked to osteoblast differentiation. This signified that the Mekk2–β-catenin axis mediated by FTZ was an imperative method to enhance osteoblast differentiation, which was independent of Wnt/β-catenin signaling. Notably, Mekk2 and Wnt shared the same objective, which was β-catenin activation. To corroborate the above discoveries further, we employed Wnt3a and FTZ alone or in combination to invigorate the TOPflash and Renilla luciferase transfected C3H10T1/2 cells, and assessed β-catenin activity by the luciferase reporter system. In comparison with stimulation with Wnt3a or FTZ, the activation of β-catenin was elevated upon treatment with the solitary ligand and FTZ. These findings signified that FTZ stimulated β-catenin by a distinct pathway dissimilar to Wnt/β-catenin signaling. The FTZ–Mekk2–β-catenin axis autonomously boosted osteoblast activity and bone formation.

5. Conclusions

Taken together, our findings suggest that FTZ exerts a protective effect against bone loss and mitigates GC-induced Wnt/β-catenin signaling via an alternative Mekk2-dependent pathway. Thus, FTZ could represent a promising therapeutic strategy for the treatment of glucocorticoid-induced osteoporosis (GIOP) by stabilizing β-catenin.

Abbreviations

GC
glucocorticoid
FTZ
Fufang Zhenshu Tiaozhi
GIOP
glucocorticoid-induced osteoporosis
Mekk2
mitogen-activated protein kinase kinase kinase 2
DXMS
dexamethasone
WT
wild type
ALP
Alkaline Phosphatase

Declarations

Ethics approval and consent to participate

The animal protocol was approved by the animal ethics broad of Guangzhou University of Chinese Medicine where the animal study was performed.

Consent for publication

Not applicable.

Availability of data and materials

The datasets used and/or analysed during the current study are available from the corresponding author on reasonable request.

Competing interests

The authors declare that they have no competing interests.

Funding

This study was supported in part by the National Natural Science Foundation of China (No. 81704098) and Guangdong Science and Technology Innovation Strategy Special Funding "Great Special Project+ Task List" (No. 2020A090402). This sponsor hasn't participated in the design of the study or collection, analysis, or interpretation of data or in writing manuscript.

Authors' contributions

Ping Sun and Qunwei Dong conceived and supervised the study; Guoju Hong designed experiments; Guoju Hong, Jiangyan Wang and Dongdong Ge performed experiments; Lin Tang provided new tools and reagents; Li Hu and Chenghong Ma analysed data; Guoju Hong wrote the manuscript; Ping Sun made manuscript revisions.

Acknowledgements

Not applicable.

Declaration of Competing Interest

None.

References

1. Buckley L, Humphrey MB, Glucocorticoid-Induced, Osteoporosis. N Engl J Med. 2018;379(26):2547–56. https://doi.org/10.1056/NEJMcp1800214.
2. Chotiyarnwong P, McCloskey EV. Pathogenesis of Glucocorticoid-Induced Osteoporosis and Options for Treatment. Nat Rev Endocrinol. 2020;16(8):437–47. https://doi.org/10.1038/s41574-020-0341-0.

3. Gregson CL, Armstrong DJ, Bowden J, Cooper C, Edwards J, Gittoes NJL, Harvey N, Kanis J, Leyland S, Low R, McCloskey E, Moss K, Parker J, Paskins Z, Poole K, Reid DM, Stone M, Thomson J, Vine N, Compston J. UK Clinical Guideline for the Prevention and Treatment of Osteoporosis. Arch Osteoporos. 2022;17(1):58. https://doi.org/10.1007/s11657-022-01061-5.
4. Adami G, Saag KG. Glucocorticoid-Induced Osteoporosis Update. Curr Opin Rheumatol. 2019;31(4):388–93. https://doi.org/10.1097/BOR.0000000000000608.
5. Watts NB. GLOW investigators. Insights from the Global Longitudinal Study of Osteoporosis in Women (GLOW). Nat Rev Endocrinol. 2014;10(7):412–22. https://doi.org/10.1038/nrendo.2014.55.
6. Silverman S, Curtis J, Saag K, Flahive J, Adachi J, Anderson F, Chapurlat R, Cooper C, Diez-Perez A, Greenspan S, Hooven F, Le Croix A, March L, Netelenbos JC, Nieves J, Pfeilschifter J, Rossini M, Roux C, Siris E, Watts N, Compston J. International Management of Bone Health in Glucocorticoid-Exposed Individuals in the Observational GLOW Study. Osteoporos Int J Establ Result Coop Eur Found Osteoporos Natl Osteoporos Found USA. 2015;26(1):419–20. https://doi.org/10.1007/s00198-014-2883-2.
7. Meszaros K, Patocs A. Glucocorticoids Influencing Wnt/β-Catenin Pathway; Multiple Sites, Heterogeneous Effects. Molecules. 2020;25(7):1489. https://doi.org/10.3390/molecules25071489.
8. Komori T. Glucocorticoid Signaling and Bone Biology. Horm Metab Res Horm Stoffwechselforschung Horm Metab. 2016;48(11):755–63. https://doi.org/10.1055/s-0042-110571.
9. Greenblatt MB, Shin DY, Oh H, Lee K-Y, Zhai B, Gygi SP, Lotinun S, Baron R, Liu D, Su B, Glimcher LH, Shim J-H. MEKK2 Mediates an Alternative β-Catenin Pathway That Promotes Bone Formation. *Proc. Natl. Acad. Sci. U. S. A.* 2016, *113* (9), E1226-1235. https://doi.org/10.1073/pnas.1600813113.
10. Yamashita M, Ying S-X, Zhang G-M, Li C, Cheng SY, Deng C-X, Zhang YE. Ubiquitin Ligase Smurf1 Controls Osteoblast Activity and Bone Homeostasis by Targeting MEKK2 for Degradation. Cell. 2005;121(1):101–13. https://doi.org/10.1016/j.cell.2005.01.035.
11. Lawson LY, Brodt MD, Migotsky N, Chermside-Scabbo CJ, Palaniappan R, Silva MJ. Osteoblast-Specific Wnt Secretion Is Required for Skeletal Homeostasis and Loading-Induced Bone Formation in Adult Mice. J Bone Miner Res Off J Am Soc Bone Miner Res. 2022;37(1):108–20. https://doi.org/10.1002/jbmr.4445.
12. Karner CM, Long F. Wnt Signaling and Cellular Metabolism in Osteoblasts. Cell Mol Life Sci CMLS. 2017;74(9):1649–57. https://doi.org/10.1007/s00018-016-2425-5.
13. Chen X, Wang J, Tang L, Ye Q, Dong Q, Li Z, Hu L, Ma C, Xu J, Sun P. The Therapeutic Effect of Fufang Zhenshu Tiaozhi (FTZ) on Osteoclastogenesis and Ovariectomized-Induced Bone Loss: Evidence from Network Pharmacology, Molecular Docking and Experimental Validation. Aging. 2022;14(14):5727–48. https://doi.org/10.18632/aging.204172.
14. Luo D, Li J, Chen K, Rong X, Guo J. Untargeted Metabolomics Reveals the Protective Effect of Fufang Zhenshu Tiaozhi (FTZ) on Aging-Induced Osteoporosis in Mice. Front Pharmacol. 2018;9:1483. https://doi.org/10.3389/fphar.2018.01483.

15. Huang X, Zhan H, Yang J, Peng L, Piao S, Wang L, Lan T, Rong X, Guo J. Long-Term Effect of Zhenzhu Tiaozhi Capsule (FTZ) on Hyperlipidemia: 2-Year Results from a Retrospective Study Using Electronic Medical Records. *Evid.-Based Complement. Altern. Med. ECAM* 2021, *2021*, 6264414. https://doi.org/10.1155/2021/6264414.
16. Luo D, Chen K, Li J, Fang Z, Pang H, Yin Y, Rong X, Guo J. Gut Microbiota Combined with Metabolomics Reveals the Metabolic Profile of the Normal Aging Process and the Anti-Aging Effect of FuFang Zhenshu TiaoZhi(FTZ) in Mice. Biomed Pharmacother Biomedecine Pharmacother. 2020;121:109550. https://doi.org/10.1016/j.biopha.2019.109550.
17. Diao H, Cheng J, Huang X, Huang B, Shao X, Zhao J, Lan D, Zhu Q, Yan M, Zhang Y, Rong X, Guo J. The Chinese Medicine Fufang Zhenzhu Tiaozhi Capsule Protects against Atherosclerosis by Suppressing EndMT via Modulating Akt1/β-Catenin Signaling Pathway. J Ethnopharmacol. 2022;293:115261. https://doi.org/10.1016/j.jep.2022.115261.
18. Wang H, Tan H, Zhan W, Song L, Zhang D, Chen X, Lin Z, Wang W, Yang Y, Wang L, Bei W, Guo J. Molecular Mechanism of Fufang Zhenzhu Tiaozhi Capsule in the Treatment of Type 2 Diabetes Mellitus with Nonalcoholic Fatty Liver Disease Based on Network Pharmacology and Validation in Minipigs. J Ethnopharmacol. 2021;274:114056. https://doi.org/10.1016/j.jep.2021.114056.
19. Guo J, Bei W, Hu Y, Tang C, He W, Liu X, Huang L, Cao Y, Hu X, Zhong X, Cao L. A New TCM Formula FTZ Lowers Serum Cholesterol by Regulating HMG-CoA Reductase and CYP7A1 in Hyperlipidemic Rats. J Ethnopharmacol. 2011;135(2):299–307. https://doi.org/10.1016/j.jep.2011.03.012.
20. Xu Y, Tang J, Guo Q, Xu Y, Yan K, Wu L, Xie K, Zhu A, Rong X, Ye D, Guo J. Traditional Chinese Medicine Formula FTZ Protects against Polycystic Ovary Syndrome through Modulating Adiponectin-Mediated Fat-Ovary Crosstalk in Mice. J Ethnopharmacol. 2021;268:113587. https://doi.org/10.1016/j.jep.2020.113587.
21. Komori T. Animal Models for Osteoporosis. Eur J Pharmacol. 2015;759:287–94. https://doi.org/10.1016/j.ejphar.2015.03.028.
22. Lane NE, Glucocorticoid-Induced, Osteoporosis. New Insights into the Pathophysiology and Treatments. Curr Osteoporos Rep. 2019;17(1):1–7. https://doi.org/10.1007/s11914-019-00498-x.
23. Canalis E, Mazziotti G, Giustina A, Bilezikian JP. Glucocorticoid-Induced Osteoporosis: Pathophysiology and Therapy. Osteoporos Int J Establ Result Coop Eur Found Osteoporos Natl Osteoporos Found USA. 2007;18(10):1319–28. https://doi.org/10.1007/s00198-007-0394-0.
24. Kenkre JS, Bassett J. The Bone Remodelling Cycle. Ann Clin Biochem. 2018;55(3):308–27. https://doi.org/10.1177/0004563218759371.
25. An J, Yang H, Zhang Q, Liu C, Zhao J, Zhang L, Chen B. Natural Products for Treatment of Osteoporosis: The Effects and Mechanisms on Promoting Osteoblast-Mediated Bone Formation. Life Sci. 2016;147:46–58. https://doi.org/10.1016/j.lfs.2016.01.024.
26. Wang T, Liu Q, Tjhioe W, Zhao J, Lu A, Zhang G, Tan RX, Zhou M, Xu J, Feng HT. Therapeutic Potential and Outlook of Alternative Medicine for Osteoporosis. Curr Drug Targets. 2017;18(9):1051–68. https://doi.org/10.2174/1389450118666170321105425.

27. Jiang Y, Lu Y, Jiang X, Hu J, Li R, Liu Y, Zhu G, Rong X. Glucocorticoids Induce Osteoporosis Mediated by Glucocorticoid Receptor-Dependent and -Independent Pathways. Biomed Pharmacother Biomedecine Pharmacother. 2020;125:109979. https://doi.org/10.1016/j.biopha.2020.109979.
28. Messina OD, Vidal M, Torres JAM, Vidal LF, Arguissain C, Pereira RM, Clark P, Cerdas Perez S, Campusano C, Lazaretti-Castro M, Zerbini C, Scali JJ, Mendez Sanchez L, Peralta-Pedrero ML, Cavallo A, Valdivia Ibarra FJ, Hernandez Pérez T. Evidence Based Latin American Guidelines of Clinical Practice on Prevention, Diagnosis, Management and Treatment of Glucocorticoid Induced Osteoporosis. A 2022 Update: This Manuscript Has Been Produced under the Auspices of the Committee of National Societies (CNS) and the Committee of Scientific Advisors (CSA) of the International Osteoporosis Foundation (IOF). Aging Clin Exp Res. 2022;34(11):2591–602. https://doi.org/10.1007/s40520-022-02261-2.
29. Latifyan S, Genot MT, Klastersky J. Bisphosphonate-Related Osteonecrosis of the Jaw: A Review of the Potential Efficacy of Low-Level Laser Therapy. Support Care Cancer Off J Multinatl Assoc Support Care Cancer. 2016;24(9):3687–93. https://doi.org/10.1007/s00520-016-3139-9.
30. Janovská Z. Bisphosphonate-Related Osteonecrosis of the Jaws. A Severe Side Effect of Bisphosphonate Therapy. Acta Medica (Hradec Kralove). 2012;55(3):111–5. https://doi.org/10.14712/18059694.2015.47.
31. Jiang L, Dong J, Wei J, Liu L. Comparison of Denosumab and Oral Bisphosphonates for the Treatment of Glucocorticoid-Induced Osteoporosis: A Systematic Review and Meta-Analysis. BMC Musculoskelet Disord. 2022;23(1):1027. https://doi.org/10.1186/s12891-022-05997-0.
32. Otto S, Pautke C, Van den Wyngaert T, Niepel D, Schiødt M. Medication-Related Osteonecrosis of the Jaw: Prevention, Diagnosis and Management in Patients with Cancer and Bone Metastases. Cancer Treat Rev. 2018;69:177–87. https://doi.org/10.1016/j.ctrv.2018.06.007.
33. Butz H, Mészáros K, Likó I, Patocs A. Wnt-Signaling Regulated by Glucocorticoid-Induced miRNAs. Int J Mol Sci. 2021;22(21):11778. https://doi.org/10.3390/ijms222111778.
34. Rossini M, Gatti D, Adami S. Involvement of WNT/β-Catenin Signaling in the Treatment of Osteoporosis. Calcif Tissue Int. 2013;93(2):121–32. https://doi.org/10.1007/s00223-013-9749-z.
35. Saidak Z, Marie PJ. Strontium Signaling: Molecular Mechanisms and Therapeutic Implications in Osteoporosis. Pharmacol Ther. 2012;136(2):216–26. https://doi.org/10.1016/j.pharmthera.2012.07.009.
36. Wan L, Zou W, Gao D, Inuzuka H, Fukushima H, Berg AH, Drapp R, Shaik S, Hu D, Lester C, Eguren M, Malumbres M, Glimcher LH, Wei W. Cdh1 Regulates Osteoblast Function through an APC/C-Independent Modulation of Smurf1. Mol Cell. 2011;44(5):721–33. https://doi.org/10.1016/j.molcel.2011.09.024.

Figures

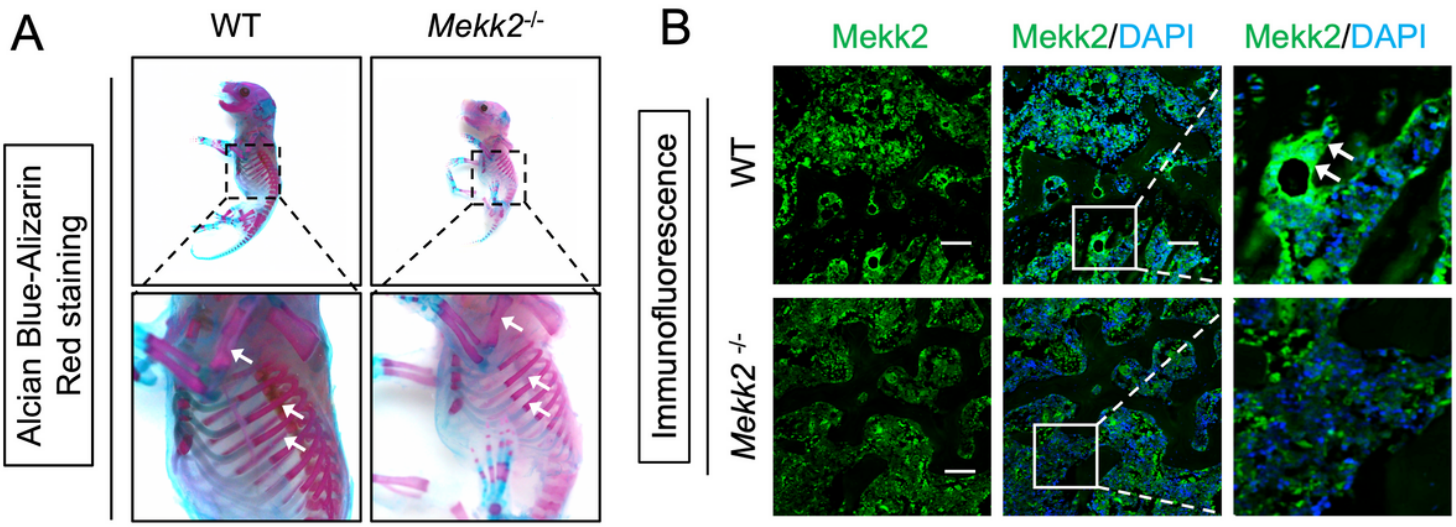

Figure 1

Knockout of *Mekk2* blocks osteogenesis and bone development. (A) Representative images show the Alcian Blue-Alizarin Red staining of fetus skeletons in WT mice and *Mekk2*$^{-/-}$ mice. White arrows indicate the phenotypic changes of limbs and ribs in fetuses. **(B)** Representative immunofluorescence images demonstrate the expression of MEKK2 on the surface of trabecula in the proximal tibiae of WT and *Mekk2*$^{-/-}$ mice. White arrows indicate the high expression of Mekk2 on the trabecula. Scale bar =100 m. WT, wild type; Mekk2, mitogen-activated protein kinase kinase kinase 2; FTZ, Fufang Zhenshu Tiaozhi capsule.

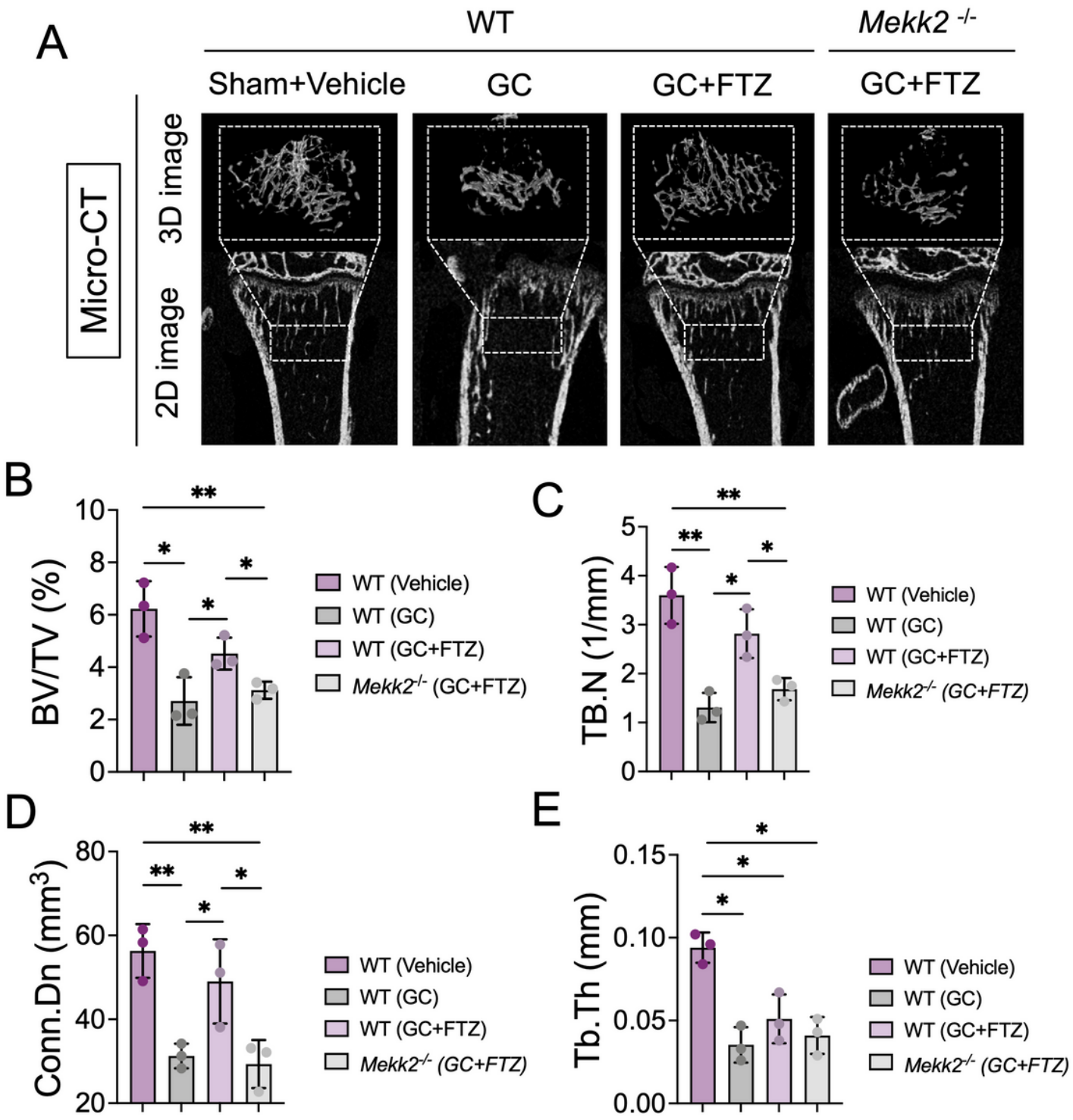

Figure 2

FTZ prevents GC-induced osteoporosis via Mekk2. (A) Representative two- and three-dimensional images detected by micro-CT show the bone mass changes of the WT, WT+DXMS, WT+DXMS+FTZ, and *Mekk2*$^{-/-}$ +DXMS+FTZ groups. **(B–E)** Quantitative analysis of microstructural parameters including BV/TV (B), Tb.N (C), Conn.Dn (D), and Tb.Th (E). *P < 0.05, **P < 0.01. BV/TV, bone volume per tissue volume; Tb.Th,

trabecular thickness; Tb.N, number of trabeculae; Conn.Dn, connectivity density; FTZ, Fufang Zhenshu Tiaozhi capsule; GC, glucocorticoid (dexamethasone).

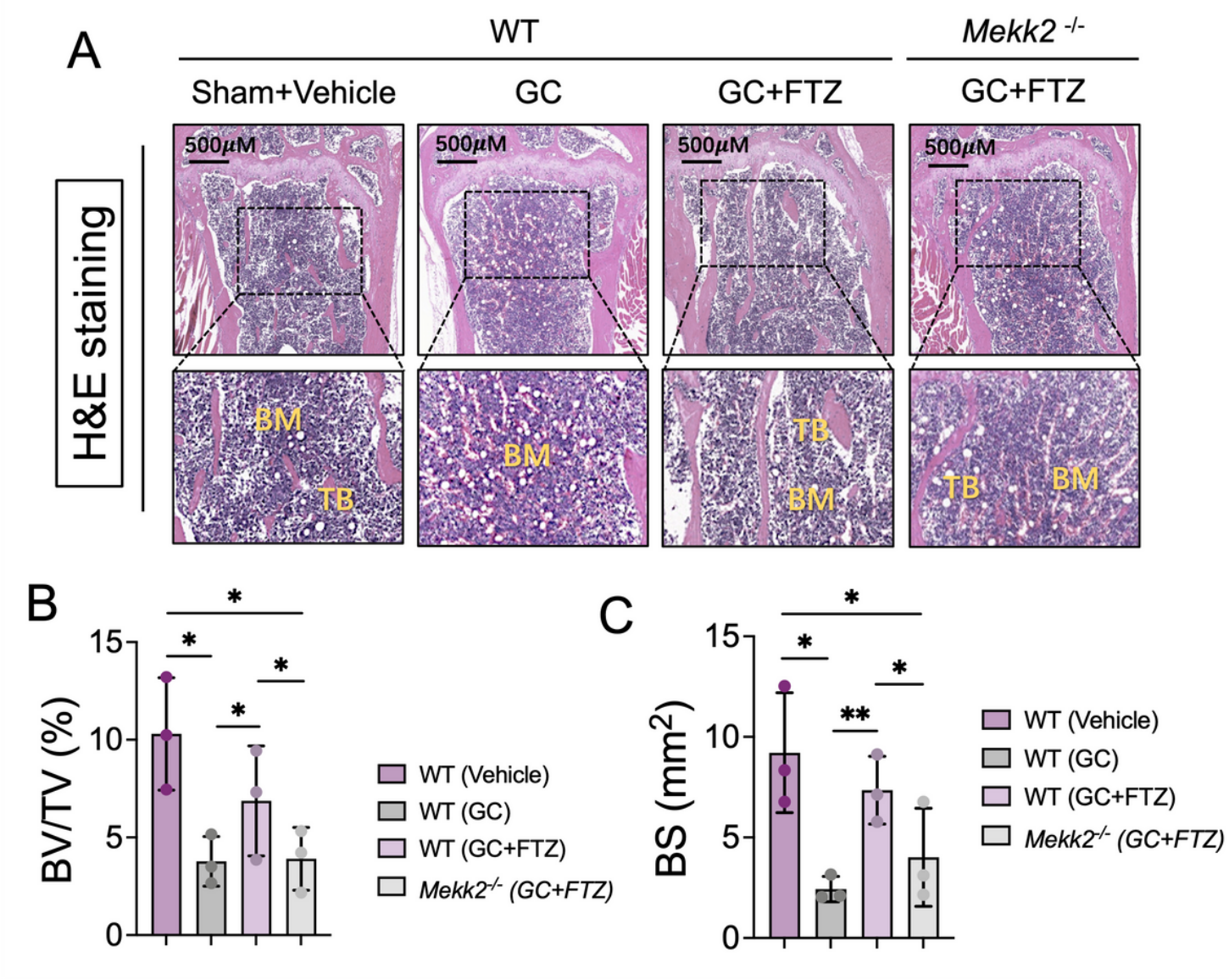

Figure 3

FTZ rescues 0bone loss in GIOP model through Mekk2. (A) Representative images detected by histomorphology analysis show the bone mass changes of the WT, WT+DXMS, WT+DXMS+FTZ, and *Mekk2*$^{-/-}$+DXMS+FTZ groups. **(B)** Quantitative analysis of microstructural parameters, including BV/TV and BS. **P* < 0.05, ***P* < 0.01. Scale bar = 500 m. BV/TV, bone volume per tissue volume; BS, bone surface; GIOP, glucocorticoid-induced osteoporosis; FTZ, Fufang Zhenshu Tiaozhi capsule; GC, glucocorticoid (dexamethasone) .

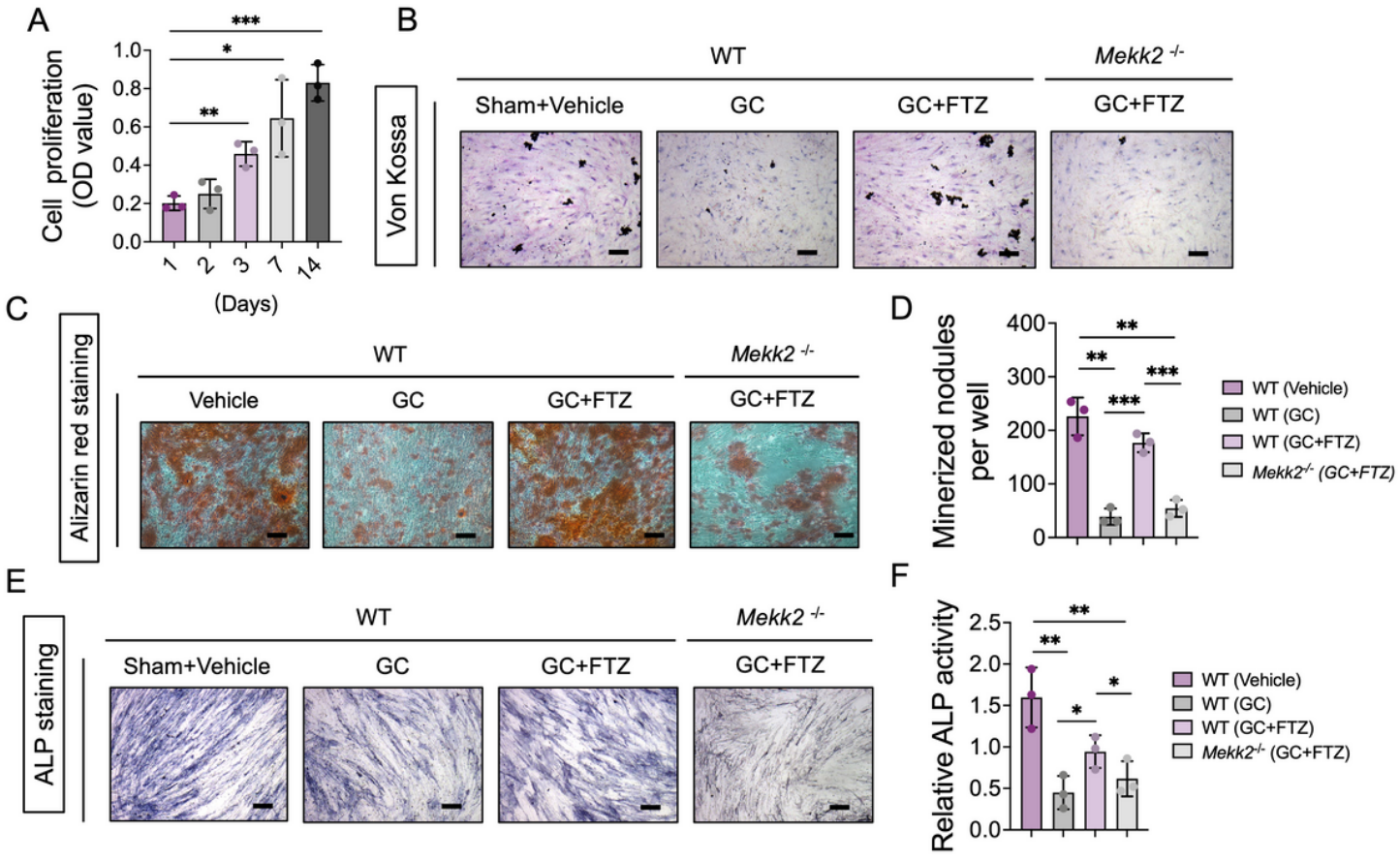

Figure 4

FTZ promotes osteogenesis differentiation by regulating Mekk2. (A) Quantitative analysis of the effects of FTZ on osteoblast proliferation from day 1 to day 14. **(B)** Representative Von Kossa images demonstrate the bone nodule formation of osteoblasts in the WT, WT+DXMS, WT+DXMS+FTZ, and *Mekk2*$^{-/-}$+DXMS+FTZ groups. **(C)** Representative images show the formation of mineralized nodules during osteoblast differentiation, as detected by Alizarin Red staining, in the WT, WT+DXMS, WT+DXMS+FTZ, and *Mekk2*$^{-/-}$+DXMS+FTZ groups. **(D)** Quantitative analysis of mineralized nodules by Alizarin Red staining. **(E)** Representative images show osteoblasts by ALP staining in the WT, WT+DXMS, WT+DXMS+FTZ, and *Mekk2*$^{-/-}$+DXMS+FTZ groups. **(F)** Quantitative analysis of ALP staining intensity. *P < 0.05, **P < 0.01. Scale bar = 100 m. FTZ, Fufang Zhenshu Tiaozhi capsule; GC, glucocorticoid (dexamethasone).

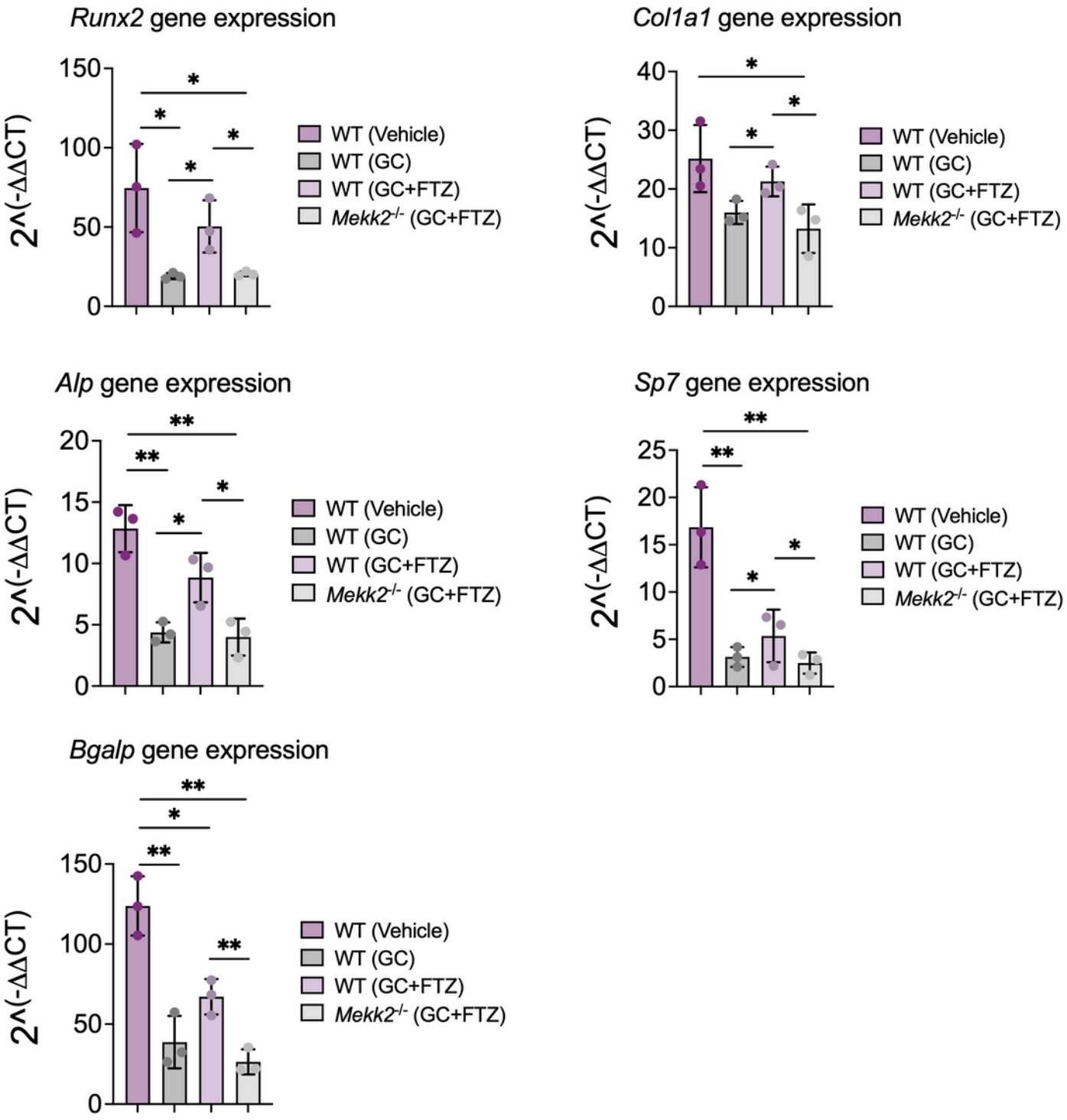

Figure 5

FTZ promotes OIM-induced gene expression in osteoblasts. RT-pPCR was used to evaluate the expression of osteoblast-related genes in OIM-induced primary cells planted with FTZ in the presence or absence of GC. Gene expression was normalized to *Gapdh*. (* $P<0.05$, ** $P<0.01$). FTZ, Fufang Zhenshu Tiaozhi capsule; GC, glucocorticoid (dexamethasone).

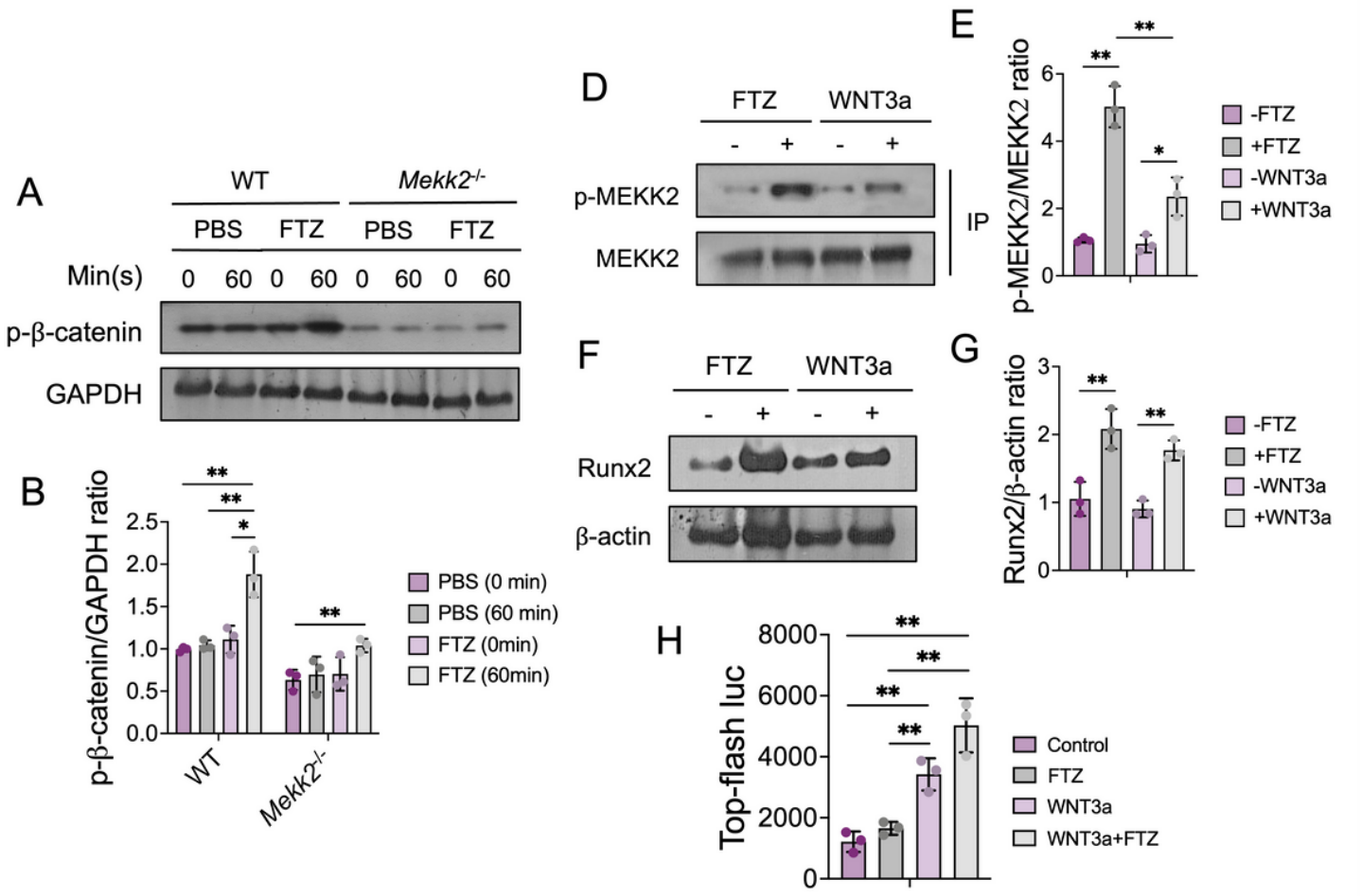

Figure 6

FTZ promotes β-catenin deubiquitination by regulating Mekk2. **(A)** Representative Western blot images show the expression of p-β-catenin in osteoblasts isolated from WT and *Mekk2*$^{-/-}$ mice in the presence or absence of FTZ. **(B)** Quantitative analysis of p-β-catenin levels normalized to β-catenin. **(C)** Quantitative analysis of p-β-catenin levels normalized to GAPDH. **(D)** Representative immunoprecipitation images show p-Mekk levels in primary osteoblasts isolated from WT mice in the presence or absence of FTZ or Wnt3a. **(E)** Quantitative analysis of p-Mekk2 levels normalized to Mekk2. **(F)** Representative Western blot images show the Runx2 levels in primary osteoblasts isolated from WT mice in the presence or absence of FTZ or Wnt3a. **(G)** Quantitative analysis of Runx2 protein levels normalized to β-actin. **(H)** C3H10T1/2 cells were transfected with TOPflash-luciferase and Renilla, and the cells were stimulated with FTZ and Wnt3a for 24 h. Luciferase activity was measured subsequently and normalized to Renilla. **P* < 0.05, ***P* < 0.01. FTZ, Fufang Zhenshu Tiaozhi capsule.

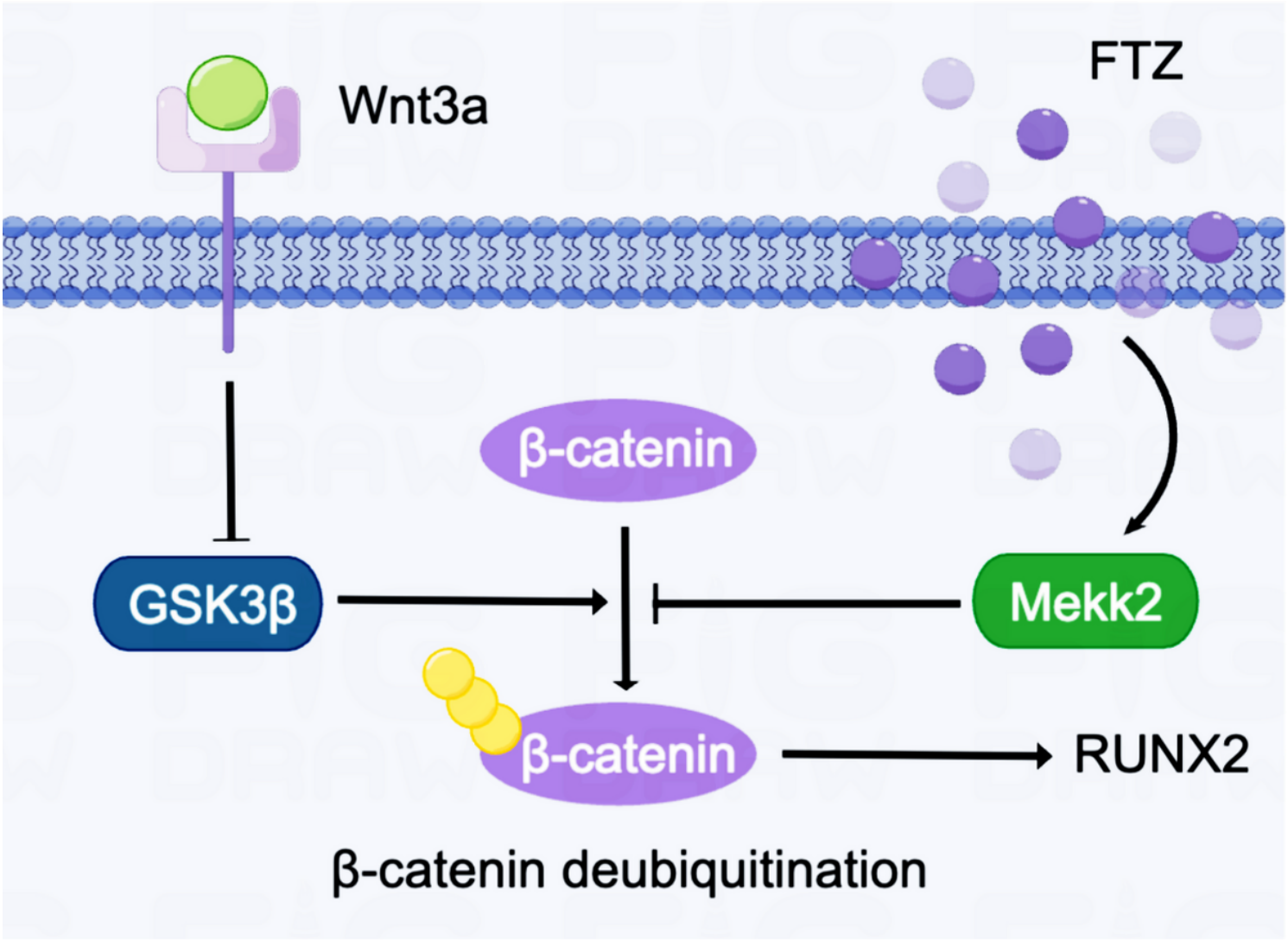

Figure 7

Schematic diagram for the molecular regulation of FTZ on Mekk2 during osteoblastogenesis.